Supplementary Information (SI) for New Journal of Chemistry.

(Supporting Information)

Efficient electrocatalytic water oxidation by N-Phthaloyl-γ-aminobutyric acid-Cobalt 1D MOF

Milan Gumtya,[a] Ayan Mondal,[a] Rahul Banerjee*[a,b] and Debasish Haldar*[a,b]

[a]Department of Chemical Science, Indian Institute of Science Education and Research, Kolkata. Mohanpur 741246, India.

[b]Centre for Advanced Functional Materials (CAFM), Indian Institute of Science Education and Research, Kolkata, Mohanpur-741246, West Bengal, India.

Corresponding Author

*(D H) deba_h76@yahoo.com; deba_h76@iiserkol.ac.in

* (R B) r.banerjee@iiserkol.ac.in

Sr. No.	Contents	Page No.
Section 1	**General information**	3-5
Section 2	Synthesis of ligands 2.1 Synthesis of ligand **1** 2.2 Synthesis of ligand **2**	5-9
Section 3	Synthesis and Characterizations of **MOF 1** and **MOF 2** 3.1 Crystal data and structure refinement for **MOF 1.** 3.2 Crystal data and structure refinement for **MOF 2**. 3.3 FTIR spectrum 3.4 Thermogravimetric analysis	9-12
Section 4	Electrochemical experiments of **MOF 1** and **MOF 2** 4.1 Linear-fit plot for double layer capacitance (Cdl) calculation 4.2 Cyclic voltammograms of **MOFs** 4.3 Plot of the volume of O2 evolution with time for **MOF 2.** 4.4 The FT-IR spectra of the **MOF 2** electrocatalyst. 4.5 iR-corrected backward LSV curves of MOF 2 at different pH.	13-19

2.1 Synthesis of Ligand 1:

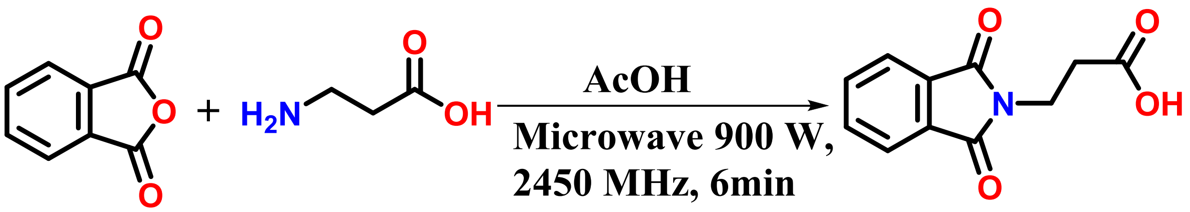

Fig. S1: Synthesis of ligand **1**.

To a solution of Phthalic anhydride (740 mg, 5mmol) in acetic acid, β-alanine (534.3 mg, 6mmol) was mixed. The reaction mixture was then stirred for 5 minutes in a micro-oven to yield a white precipitate. The obtained precipitate was further washed with water and work-up by ethyl acetate. Yield 90 %. The products were purified by column chromatography using silica (100−200 mesh size) gel as a stationary phase and an n-hexane-ethyl acetate mixture as an eluent. **^{1}H NMR** (500 MHz, DMSO, δ ppm) of ligand**:** 12.373 (s, 1H, carboxylic proton), 7.7-7.9 (m, 4H, aromatic proton), 3.79 (t, 2H, methylene proton), 2.60 (t, 2H, methylene proton). **^{13}C NMR** (125 MHz, DMSO, δ ppm) of ligand**:** (172.80, 168.1, 134.9, 132.11, 123.52, 34.14, 32.93). **ESI-MASS:** calculated 242.01, found 242.04.

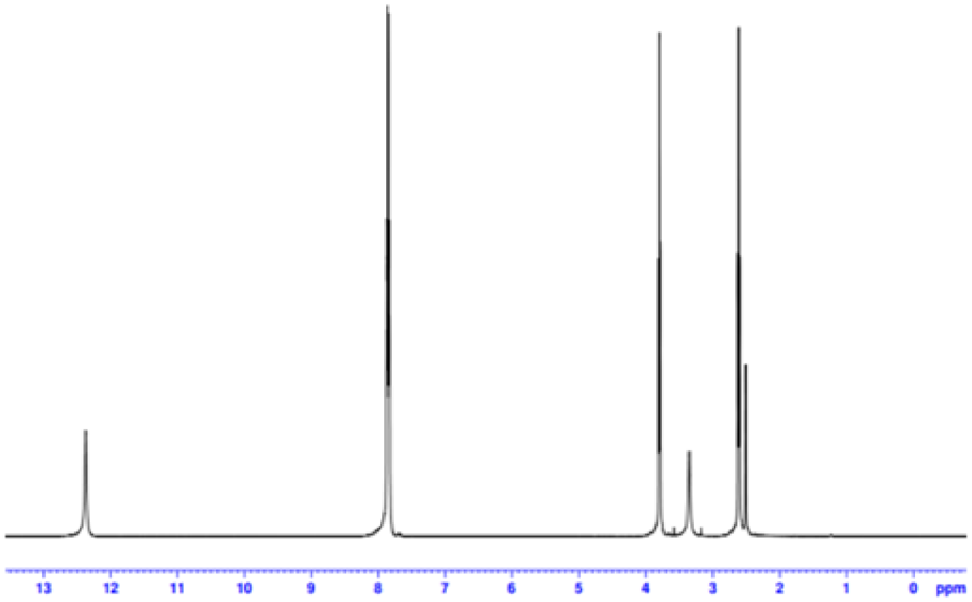

Fig. S2: ^{1}H NMR spectra of ligand **1** in DMSO-D6.

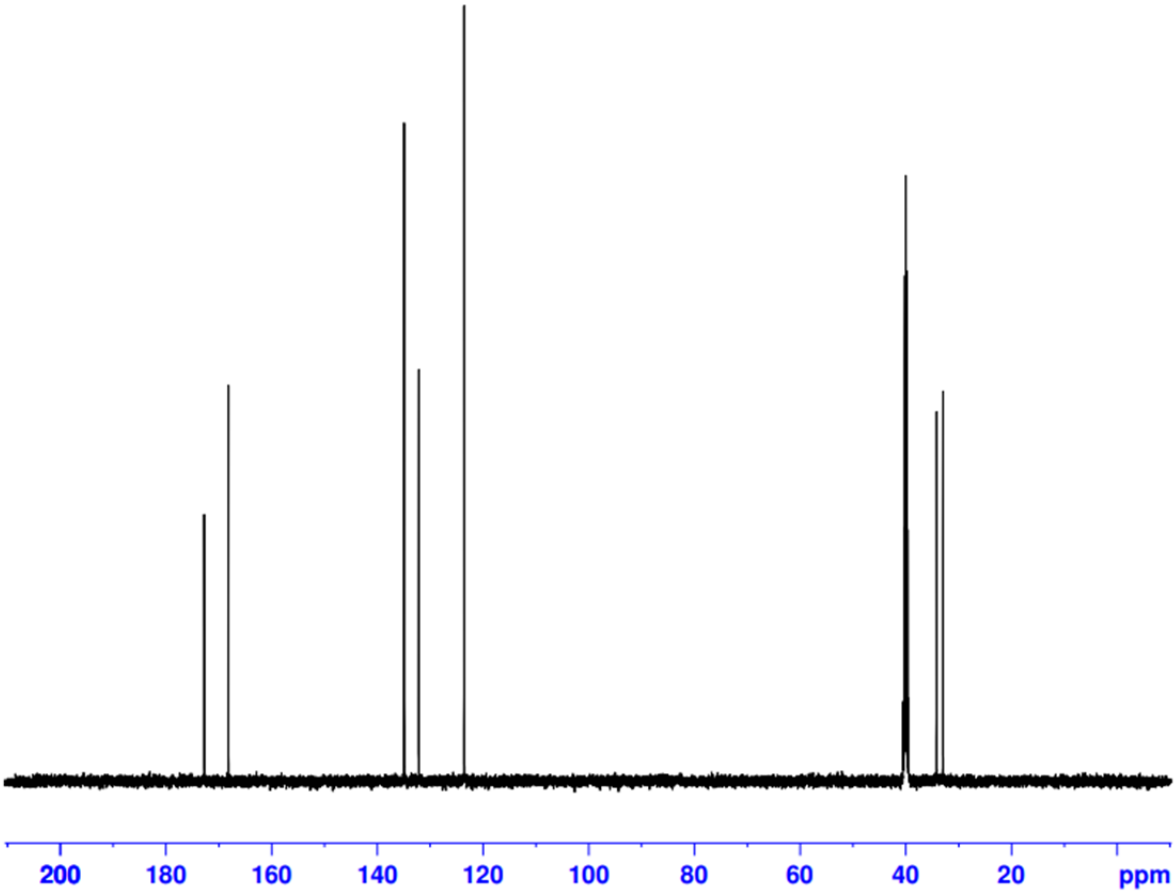

Fig. S3:^{13}C NMR spectra of ligand **1** in DMSO-d6**.**

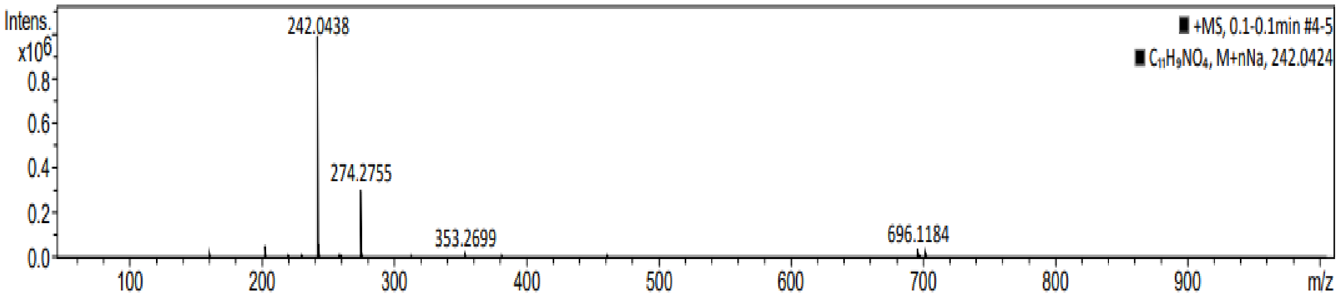

Fig. S4: ESI-MS spectra of ligand **1.**

2.2 Synthesis of Ligand 2:

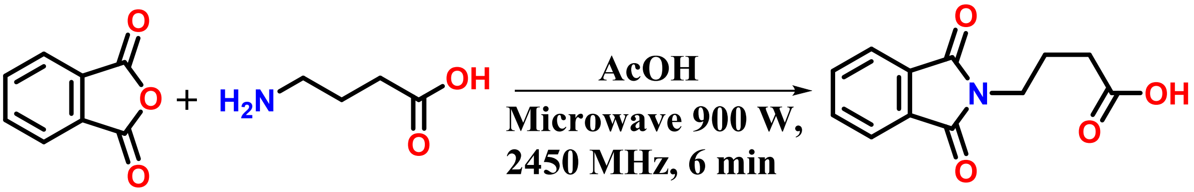

Fig. S5: Synthesis of ligand **2**.

To a solution of phthalic anhydride (740 mg, 5mmol) in acetic acid, gamma-aminobutyric acid (618.36mg, 6mmol) was added. The reaction mixture was then stirred for 5 minutes in a micro-oven to yield a white precipitate. The obtained precipitate was further washed with water and work-up by ethyl acetate. Yield 90 %. **^{1}H NMR** (500 MHz, DMSO, δ ppm) of ligand: 12.18 (s, 1H, carboxylic proton), 7.86-7.79 (m, 4H, aromatic proton), 3.60 (t, 2H, methylene proton), 2.26 (t, 2H, methylene proton), 1.81(m, 2H, methylene proton). **^{13}C NMR** (125 MHz, DMSO, δ ppm) of ligand**:** (174.30, 168.43, 134.73, 132.13, 123.4, 37.37, 31.43, 23.81). **ESI-MASS:** calculated 256.01, found 256.0598.

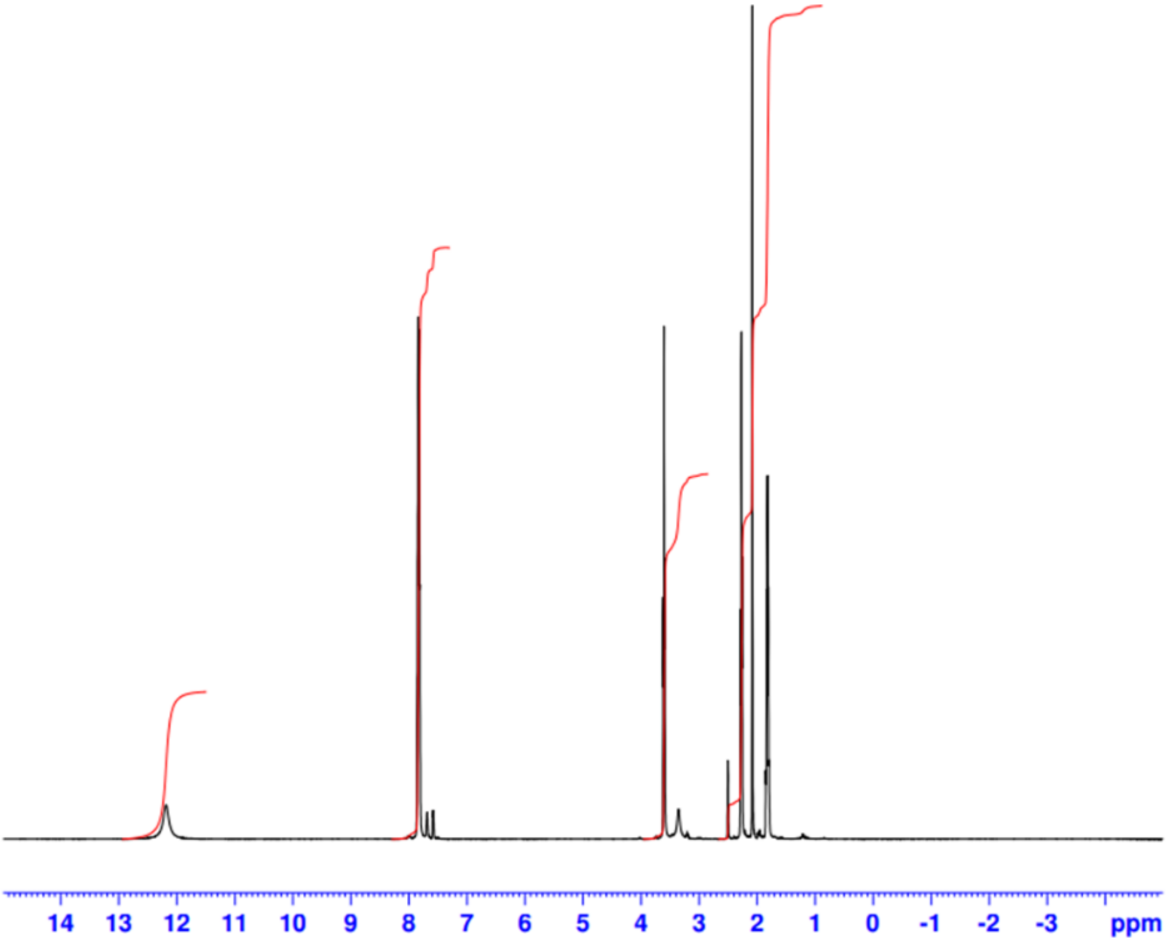

Fig. S6: ^{1}H NMR spectra of ligand **2** in DMSO-D6.

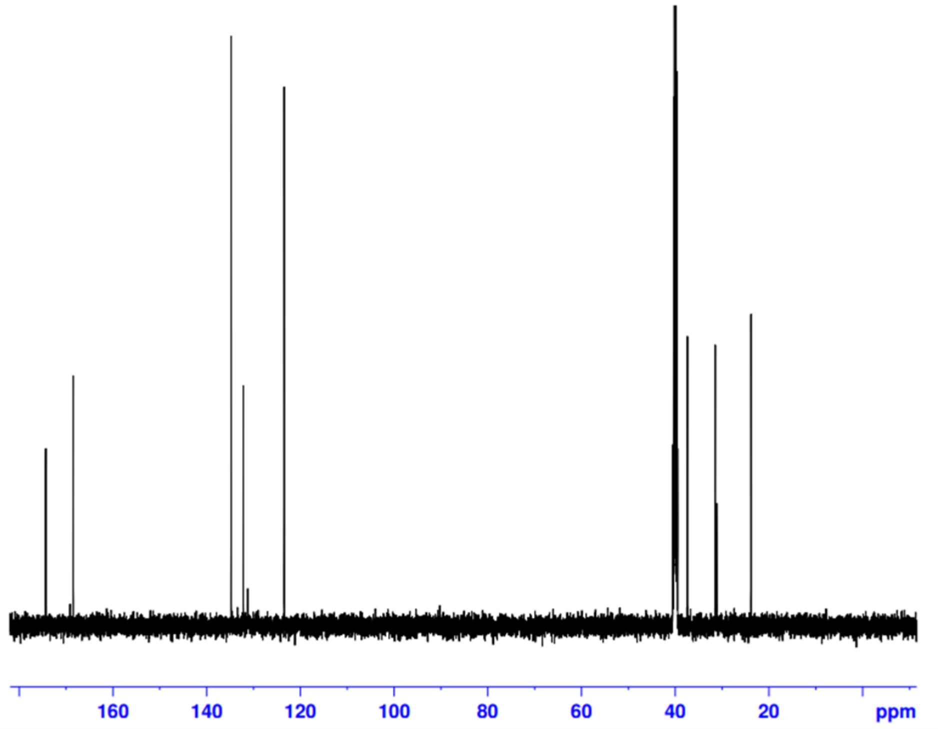

Fig. S7: ^{13}C NMR spectra of ligand **2** in DMSO-d6**.**

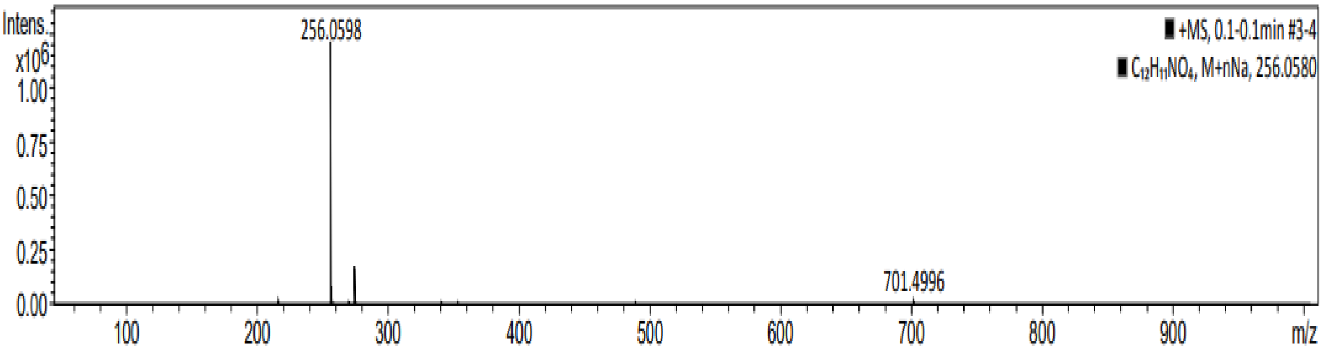

Fig. S8: ESI-MS spectra of ligand **2.**

Section 3:

Synthesis of MOF 1: An aqueous solution of cobalt (II) acetate tetrahydrate (44.25 mg, 0.25 mmol, 2.5 mL water) was added dropwise to a well-stirred solution of ligand (109.53 mg, 0.5 mmol) in ethanol (2.5 mL) at room temperature. The resulting pink color solution was stirred at room temperature for 5 hours and left undisturbed (Fig. 14). After 20 days pink color crystals were obtained within the solution. HRMS: m/z 496.09 for $[\text{Co}^{\text{II}}\text{L}_2] + 2\text{H}^+$.

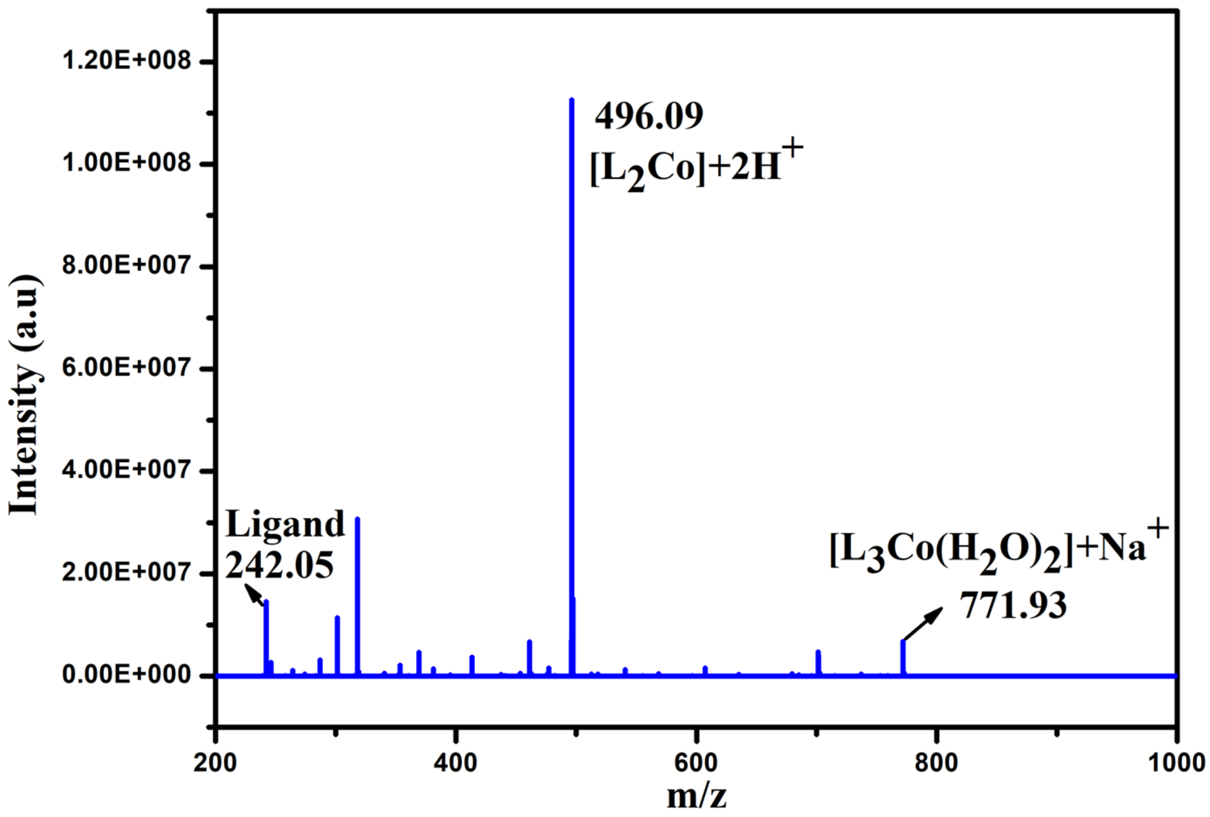

Fig. S9: ESI-MS of **MOF 1**.

3.1

Identificationcode	**MOF 1**
Empiricalformula	C22 H22 Co N2 O11, 2(C0.46 H1.46 O), 2(C H2)
Formulaweight	623.42
Temperature/K	100
Crystalsystem	monoclinic
Spacegroup	*C 2/c*
a/Å	14.4806(3)
b/Å	23.7117(7)
c/Å	8.07794(19)
α/°	90
β/°	101.305(2)
γ/°	90
Volume/Å^3	2719.82(12)
Z	4

ρ_{calc}g/cm^3	1.523
μ/mm^{-1}	5.582
F(000)	1293.8
Crystalsize/mm^3	0.35× 0.15× 0.1
Radiation	CuKα (λ = 1.54184)
2Θrange for datacollection/°	7.26 to 136.2
Flackparameter	0.0(4)
Final R indexes [all data]	R1= 0468, wR2= 0.1322

Table S1: Crystal data and structure refinement for **MOF 1.**

Synthesis of MOF 2: An aqueous solution of cobalt (II) acetate tetrahydrate (44.25 mg, 0.25 mmol, 2.5 mL water) was added dropwise to a well-stirred solution of ligand (116.5 mg, 0.5 mmol) in ethanol (2.5 mL) at room temperature. The resulting pink color solution was stirred at room temperature for 5 hours and left undisturbed. After 30 days pink color crystals were obtained within the solution. HRMS: m/z 524.02 for [Co^{II}L$_2$] + H$^+$.

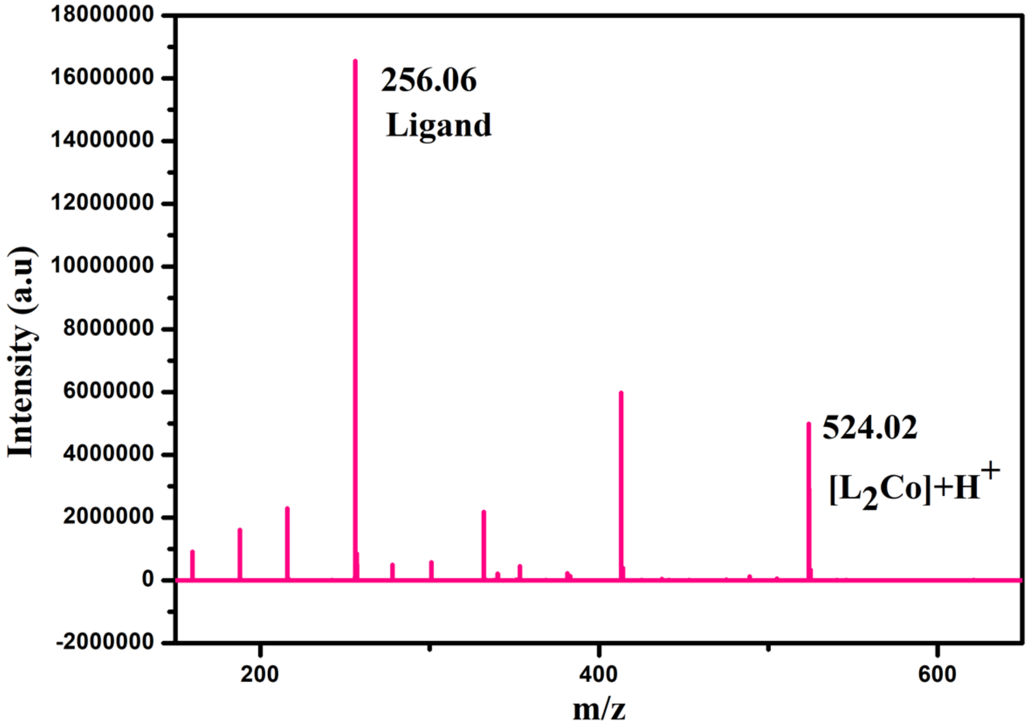

Fig. S10: ESI-MS of **MOF 2**.

3.2

Identificationcode	**MOF 2**
Empiricalformula	C24 H24 Co N2 O10, H2O
Formulaweight	577.40
Temperature/K	100
Crystalsystem	monoclinic
Spacegroup	*P 21/n*
a/Å	8.04154(11)
b/Å	15.1977(2)
c/Å	19.5905(3)
α/°	90
β/°	93.9704(13)
γ/°	90
Volume/Å^3	2388.47(6)
Z	4
ρ_{calc}g/cm^3	1.606
μ/mm^{-1}	6.241
F(000)	1196.0
Crystalsize/mm^3	0.867× 0.621× 0.423
Radiation	CuKα (λ = 1.54184)
2Θrange for datacollection/°	7.368 to 136.532
Flackparameter	0.0(4)
Final R indexes [all data]	R_1=0.0449, wR_2= 0.1259

Table S2: Crystal data and structure refinement for MOF **2**.

3.3 FTIR spectrum:

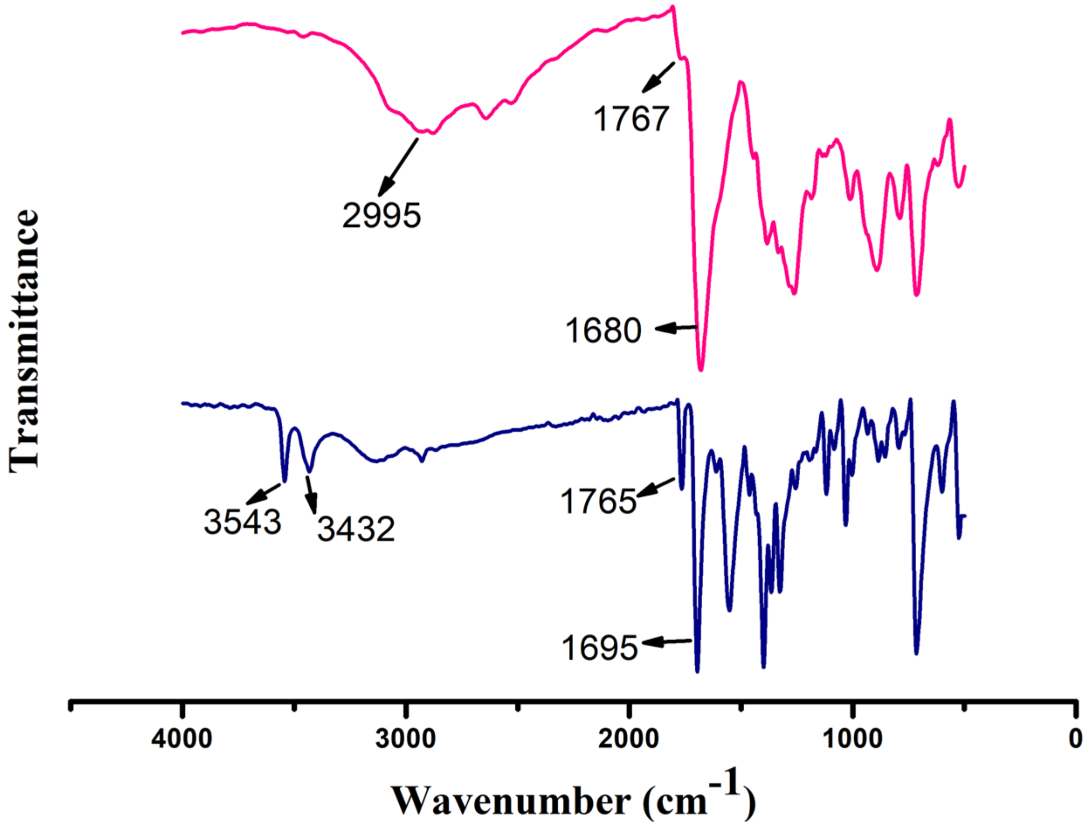

Fig. S11: FT-IR spectra of **ligand 2** (pink) and **MOF 2** (blue).

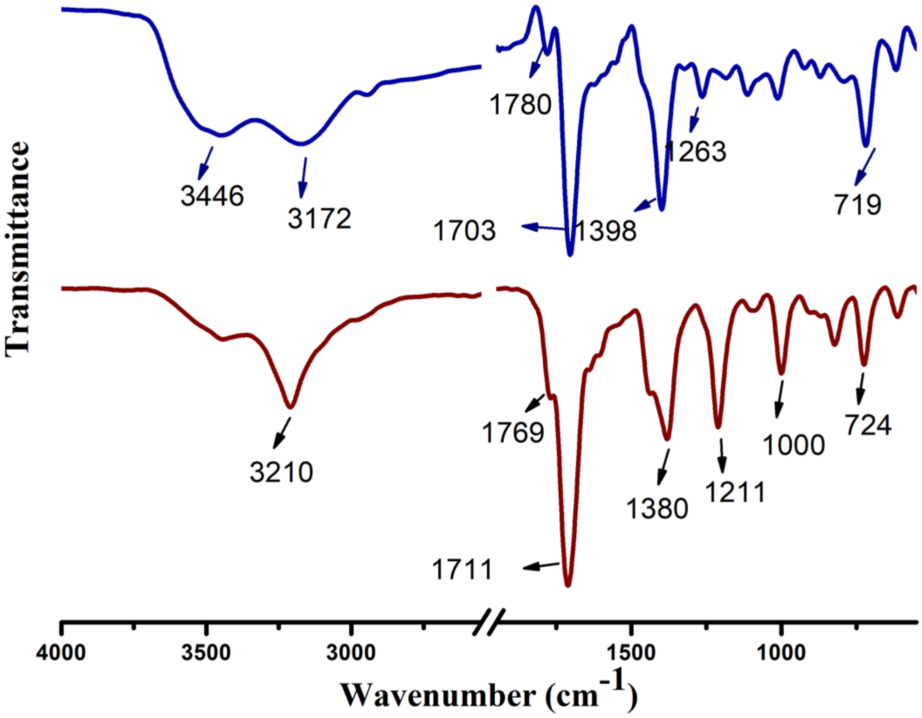

Fig. S12: FT-TR spectrum of **ligand 1** (grey) and **MOF 1**(blue).

3.4 Thermogravimetric analysis:

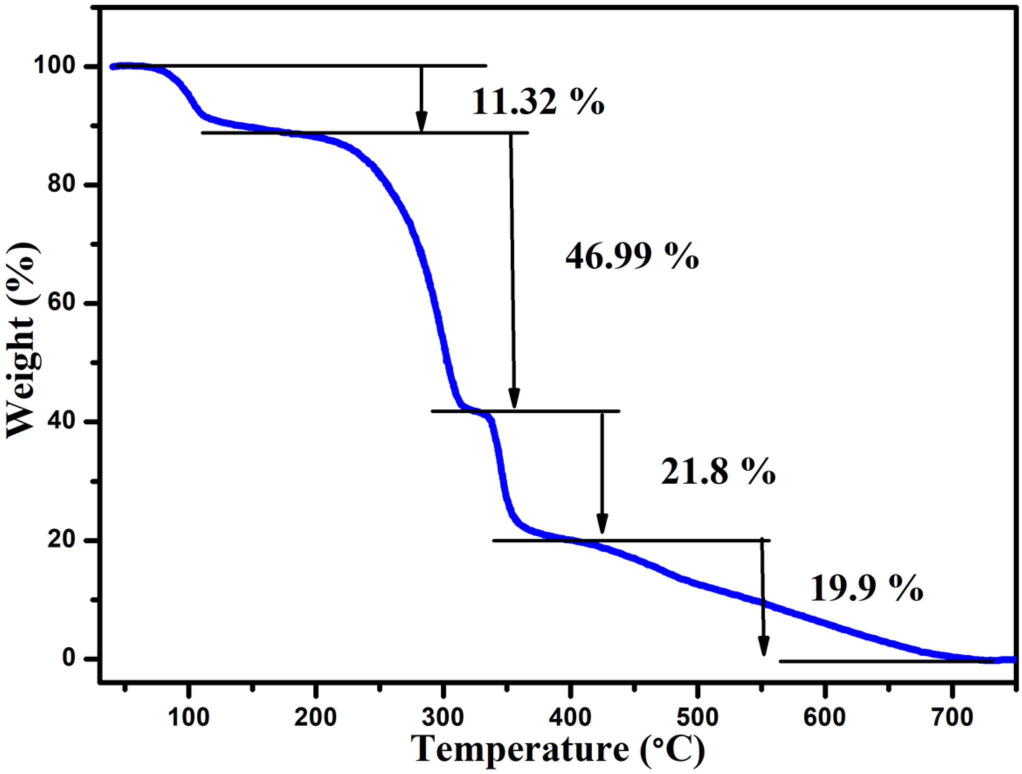

Fig. S13: Thermogravimetric analysis **MOF 1**(heating rate 10 ^{o}C per minute).

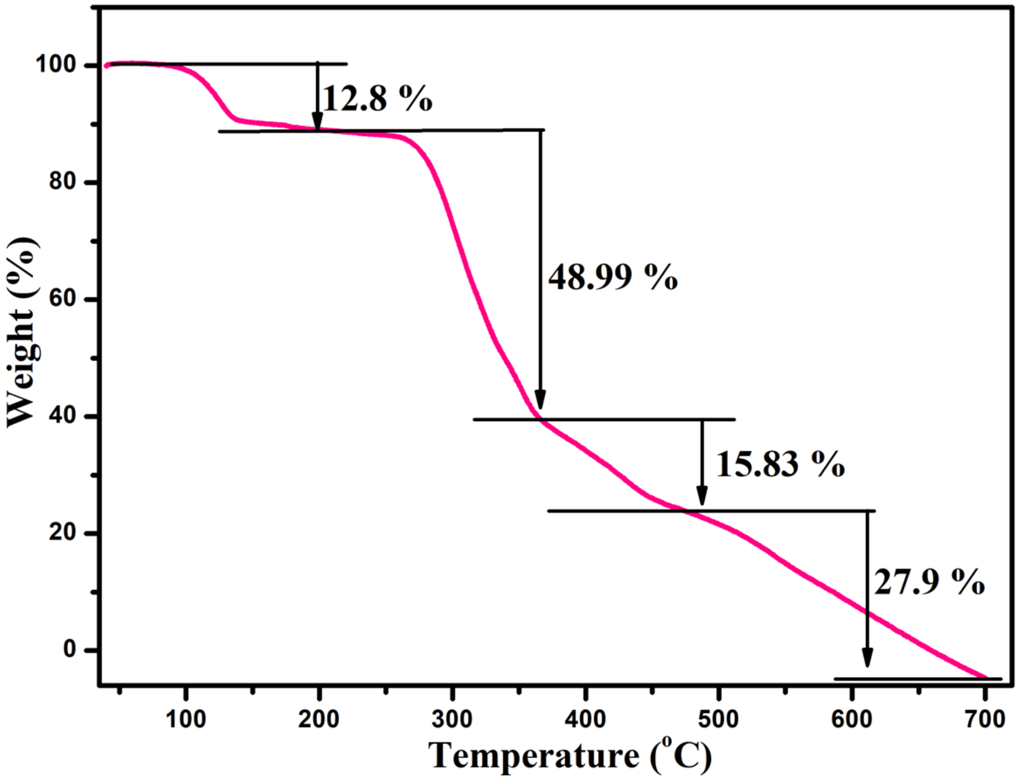

Fig. S14: Thermogravimetric analysis **MOF 2** (heating rate 10 ^{o}C per minute).

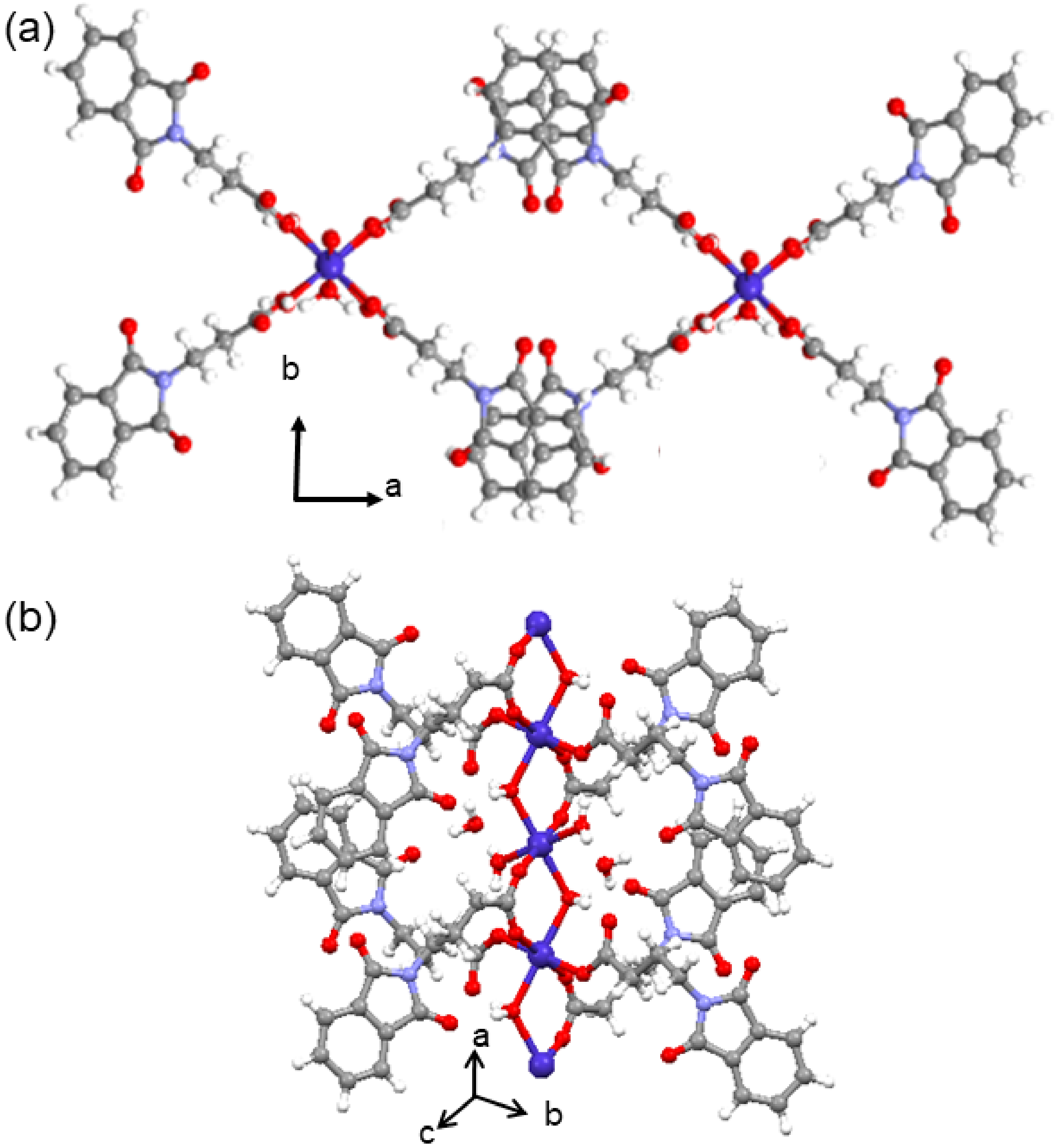

Fig. S15: (a) Packing diagram of the **MOF 1** (b) Packing diagram of the **MOF 2**.

Section 4:

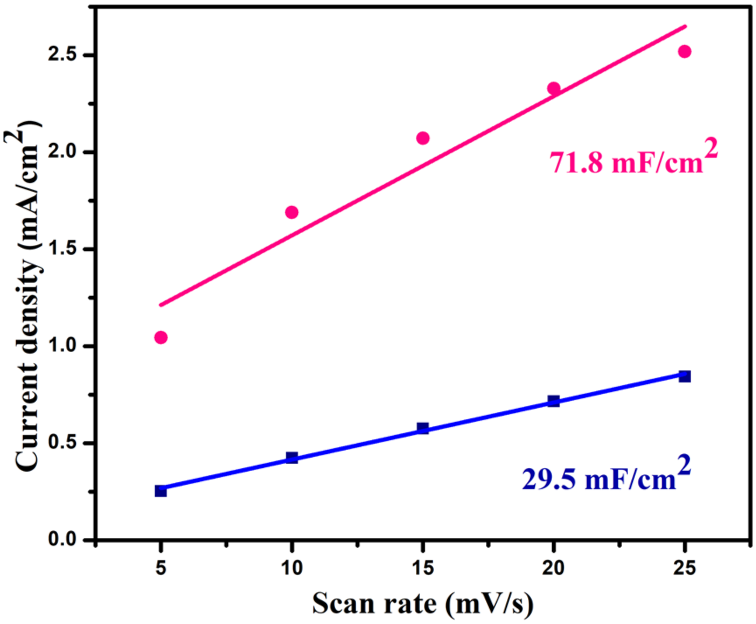

Fig. S16: Linear-fit plot for double layer capacitance (Cdl) calculation of s current vs scan rate plot for **MOF 1**(blue) and **MOF 2** (pink).

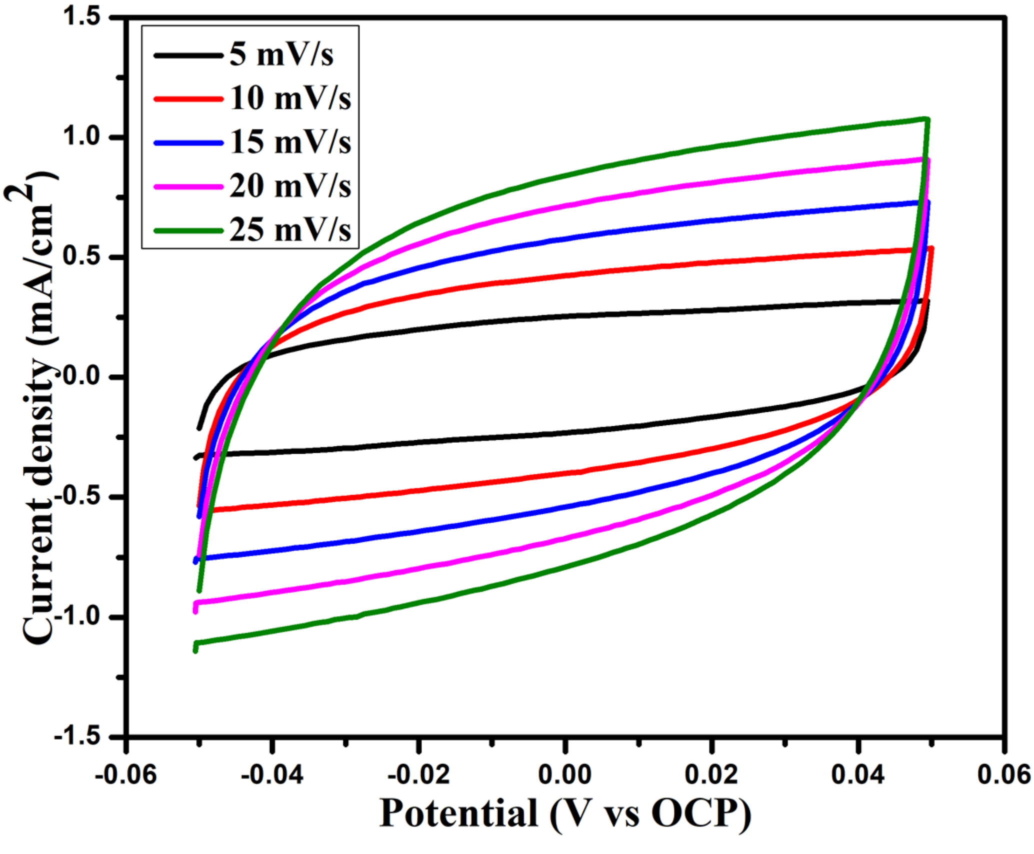

Fig. S17: Cyclic voltammograms of **MOF 1** recorded at different scan rates.

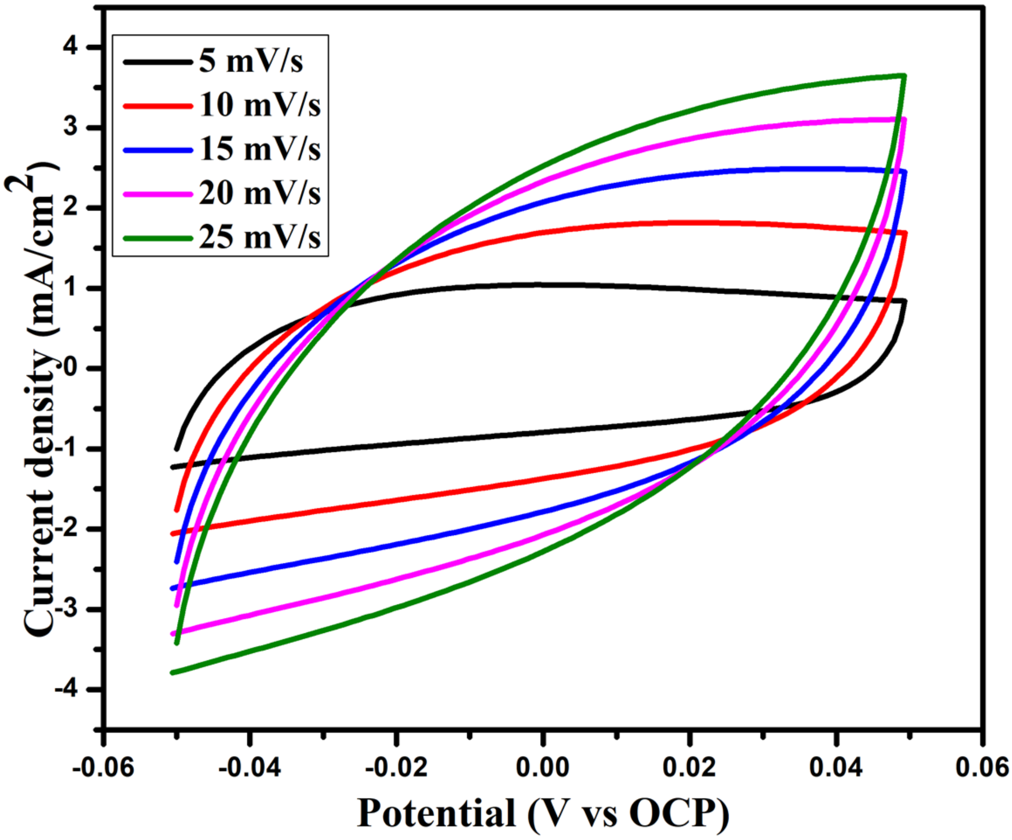

Fig. S18: Cyclic voltammograms of **MOF 2** recorded at different scan rates.

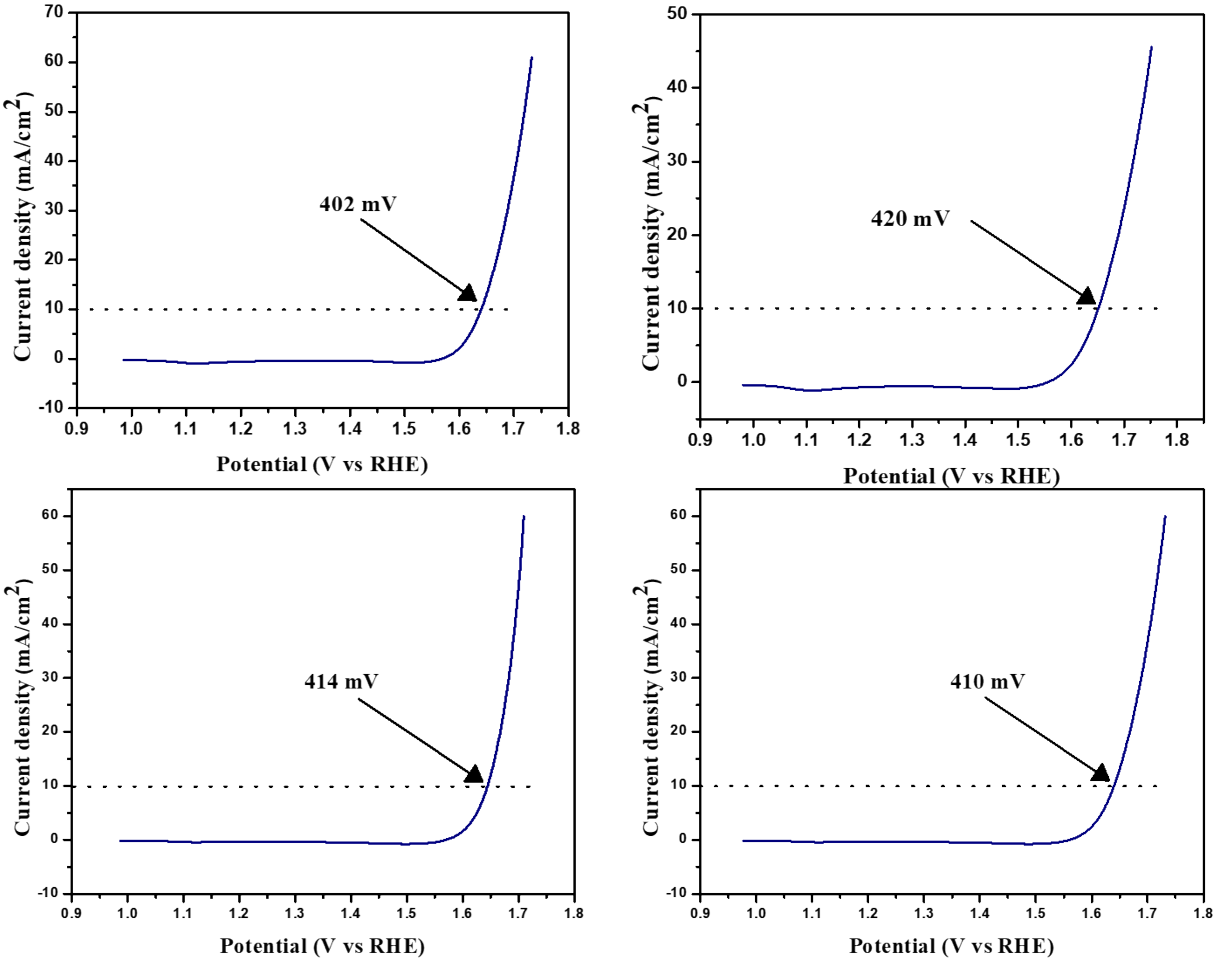

Fig. S19: LSV curves of MOF 1 recorded at different times to calculate the standard deviation.

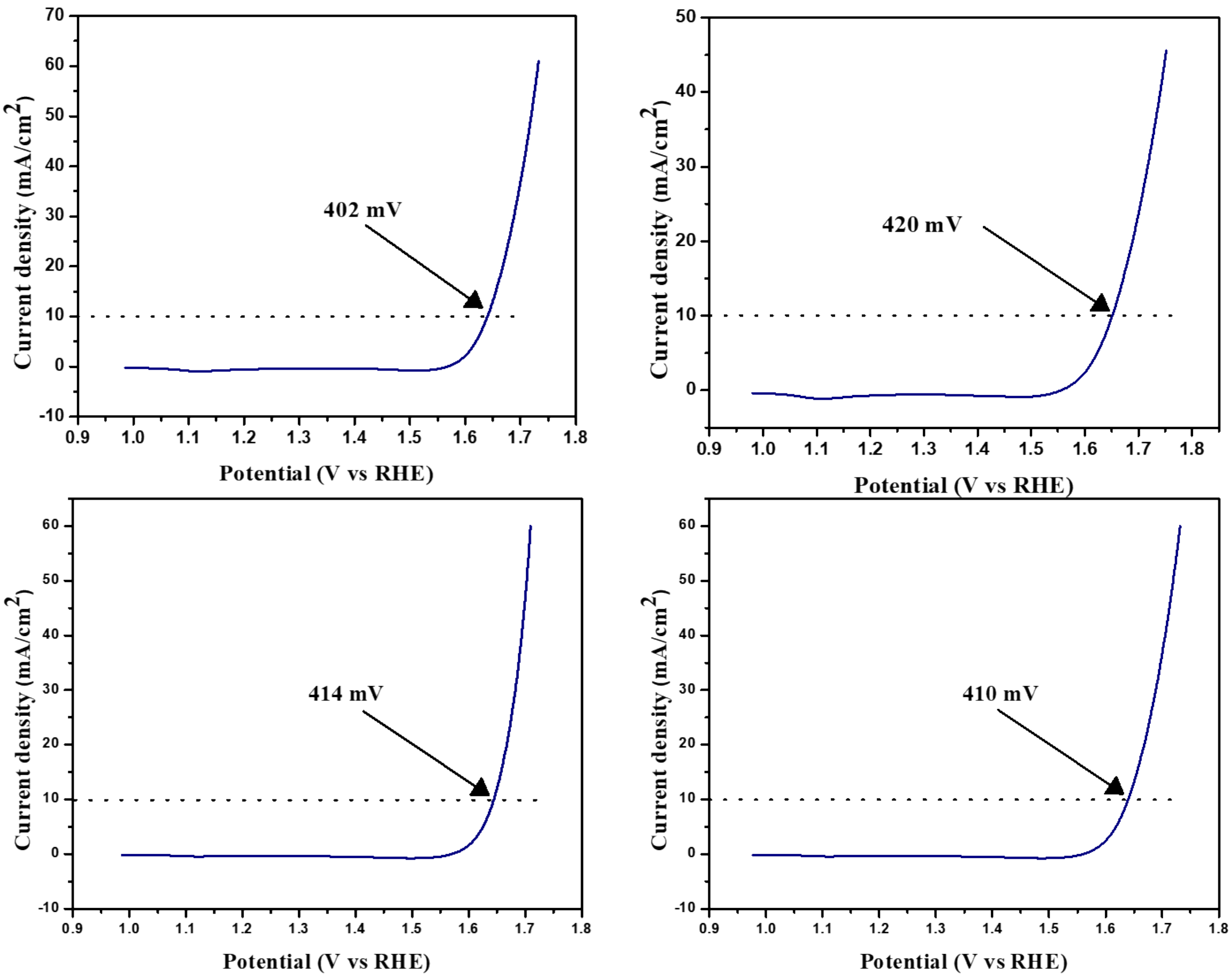

Fig. S20: LSV curves of MOF 2 recorded at different times to calculate the standard deviation.

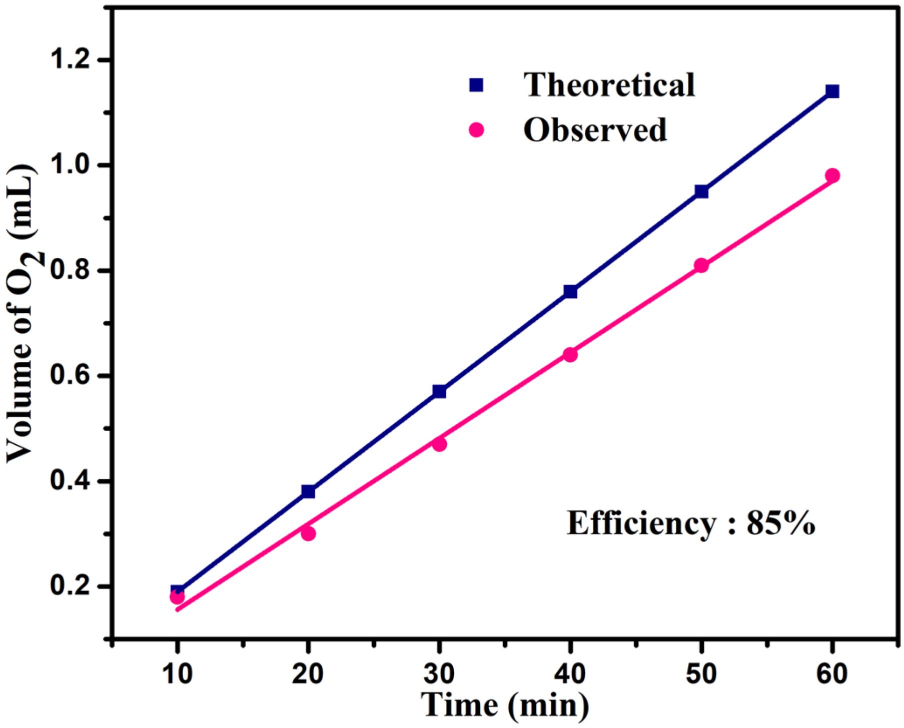

Fig. S21: Plot of the volume of O2 evolution with time for **MOF 2** sample for estimation of Faradaic efficiency.

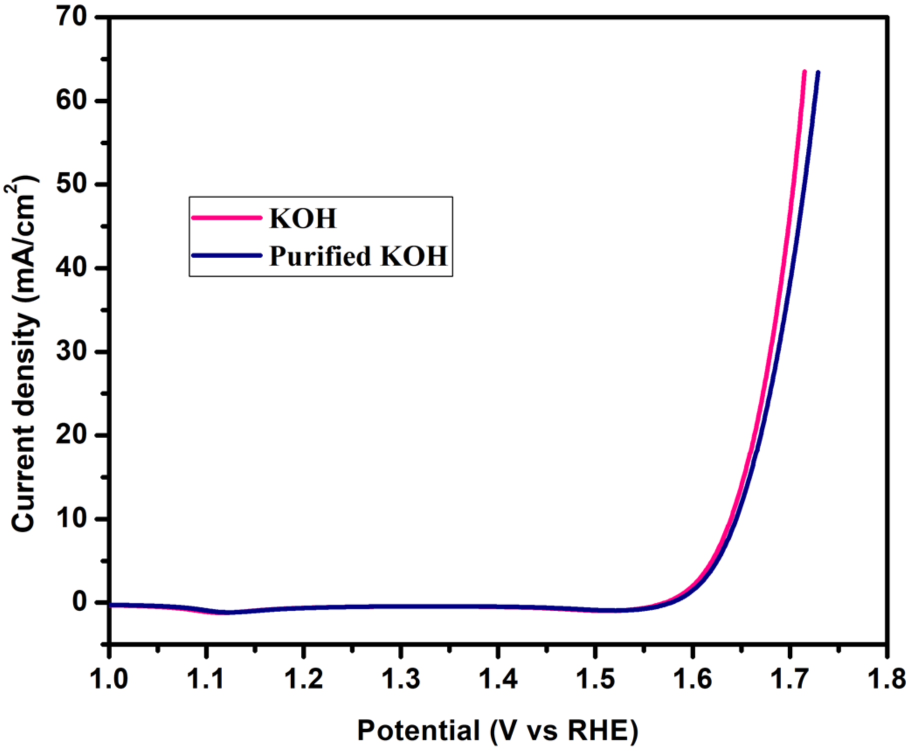

Fig. S22 : We have purified the KOH following a procedure reported by Boettcher *et al* (J. Am. Chem. Soc. 2014, 136, 6744−6753). We did no observe significant change in the activity KOH and purified KOH. .

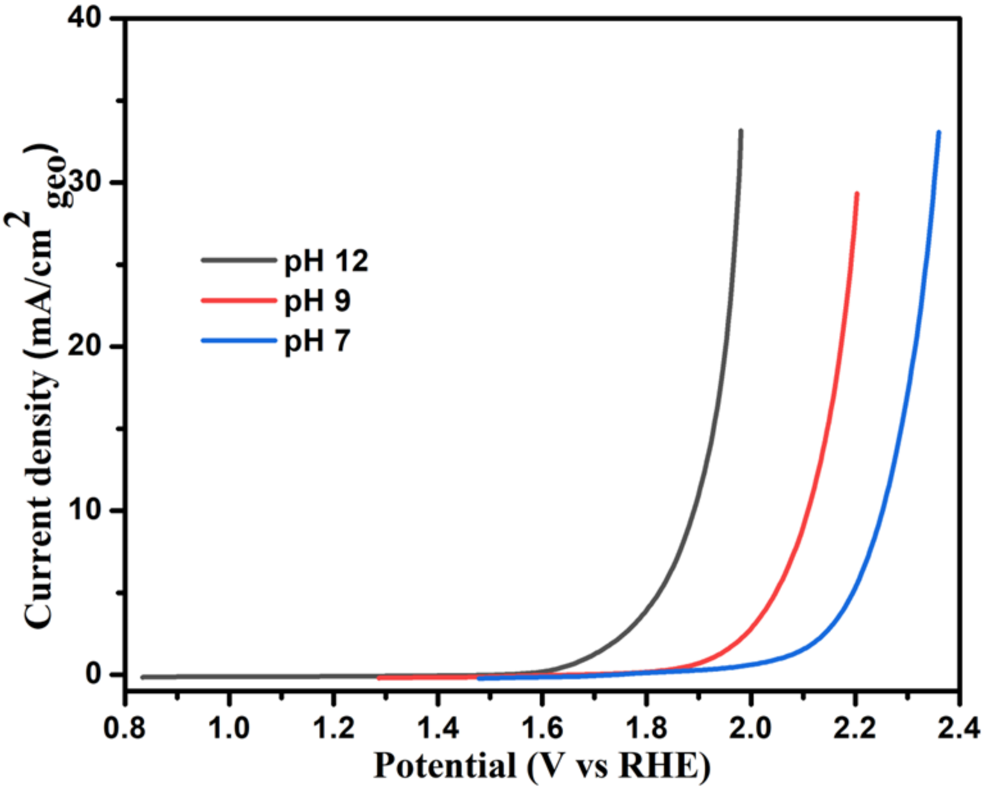

Fig. S23: iR-corrected backward LSV curves of MOF 2 at different pH.

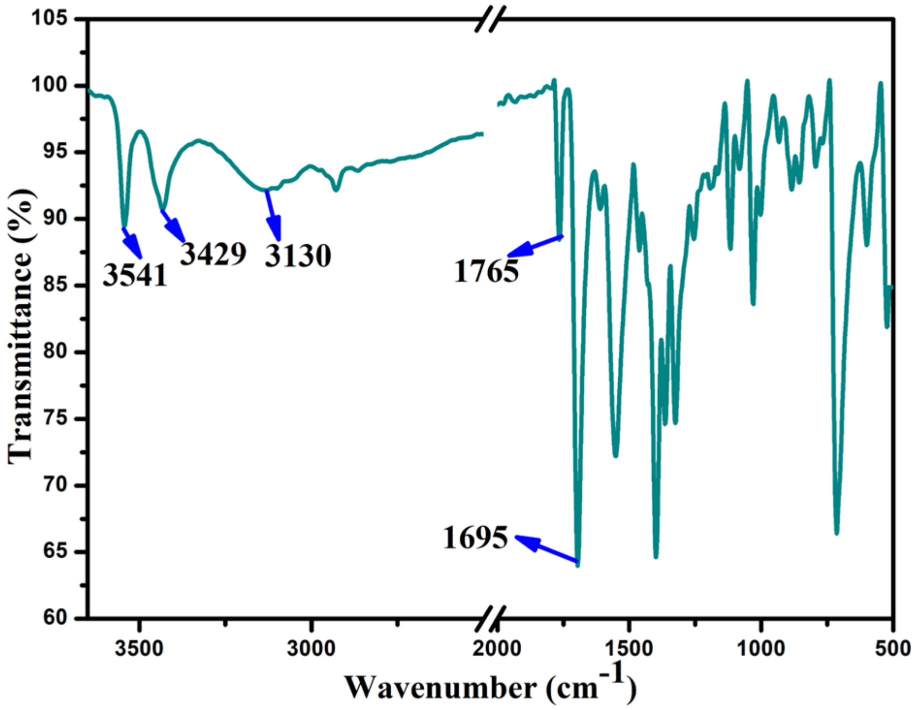

Fig. S24: The FT-IR spectra of the MOF 2 electrocatalyst was collected after the electrocatalytic stability study. The spectra displayed characteristic signals for all the functional groups as the starting materials. This result confirmed the electrocatalytic stability of the MOF **2**.

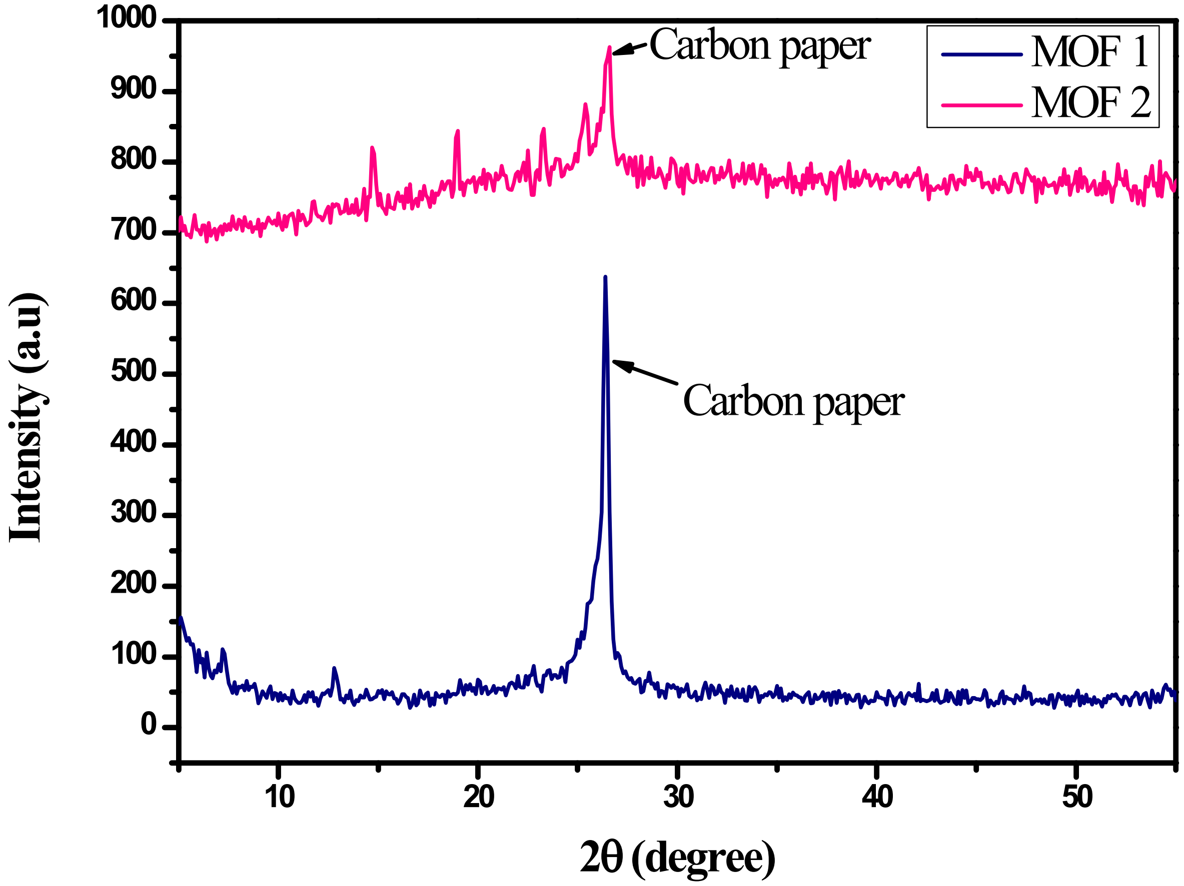

Fig. S25: PXRD patterns of post catalytic MOF 1 and MOF 2.

Element	Binding Energy (eV)	Remarks
Co	780.40(2p$_{3/2}$), 795.67 (2p$_{1/2}$) 804.22 (sat.)789.57 (sat.)	Oxidation state: II
	779.41 (2p$_{3/2}$), 794.67 (2p$_{1/2}$)	Oxidation state: III
O	528.85	Lattice oxygen in oxide environment
	530.65	Lattice oxygen in hydroxide/oxyhydroxide environment
	535.42	Adsorbed oxygen species

Table S3: XPS peak positions of Co 2p, O 1s present in MOF 1 after catalysis.

Element	Binding Energy (eV)	Remarks
Co	780.75($2p_{3/2}$), 796.77 ($2p_{1/2}$) 804.22 (sat.)789.57 (sat.)	Oxidation state: II
	779.67 ($2p_{3/2}$), 794.77 ($2p_{1/2}$)	Oxidation state: III
O	529.05	Lattice oxygen in oxide environment
	530.63	Lattice oxygen in hydroxide/oxyhydroxide environment
	531.51	Adsorbed oxygen species

Table S4: XPS peak positions of Co 2p, O 1s present in MOF 2 after catalysis.

Faradaic efficiency calculation

To assess Faradaic efficiency, catalysts were placed in a water-filled inverted burette and chronocoulometry was performed at different time intervals. The gasses created gathered atop the burets, causing a drop in water level and allowing precise measurement of gas volume. This measured volume was then compared to the theoretically expected output using chronocoulometry, allowing the Faradaic efficiency of the electrocatalyst to be determined.

We took 10-minute intervals and ($5*10^{-3}$) A current for the measurement. The calculation for determining the expected volume of O_2 evolved is as follows:

Total charge = ($5 * 10^{-3)}$ A * 600 sec = 3 Coulomb

96500 C is equivalent to 1 mol of e^-

3 C is equivalent to 3/96500 mol of e^-

In OER, 4 mol e^- is required to generate 1 mol O_2

Thus, 3/96500 mol e^- can produce $\frac{3}{96500 * 4}$ mol O_2

From the PV=nRT equation, the obtained theoretical volume of O_2 is 0.190 mL.

$$\text{The faradaic efficiency} = \frac{volume\ of\ O2\ observed\ in\ burrette}{Theoritical\ volume\ of\ O2} \times 100$$

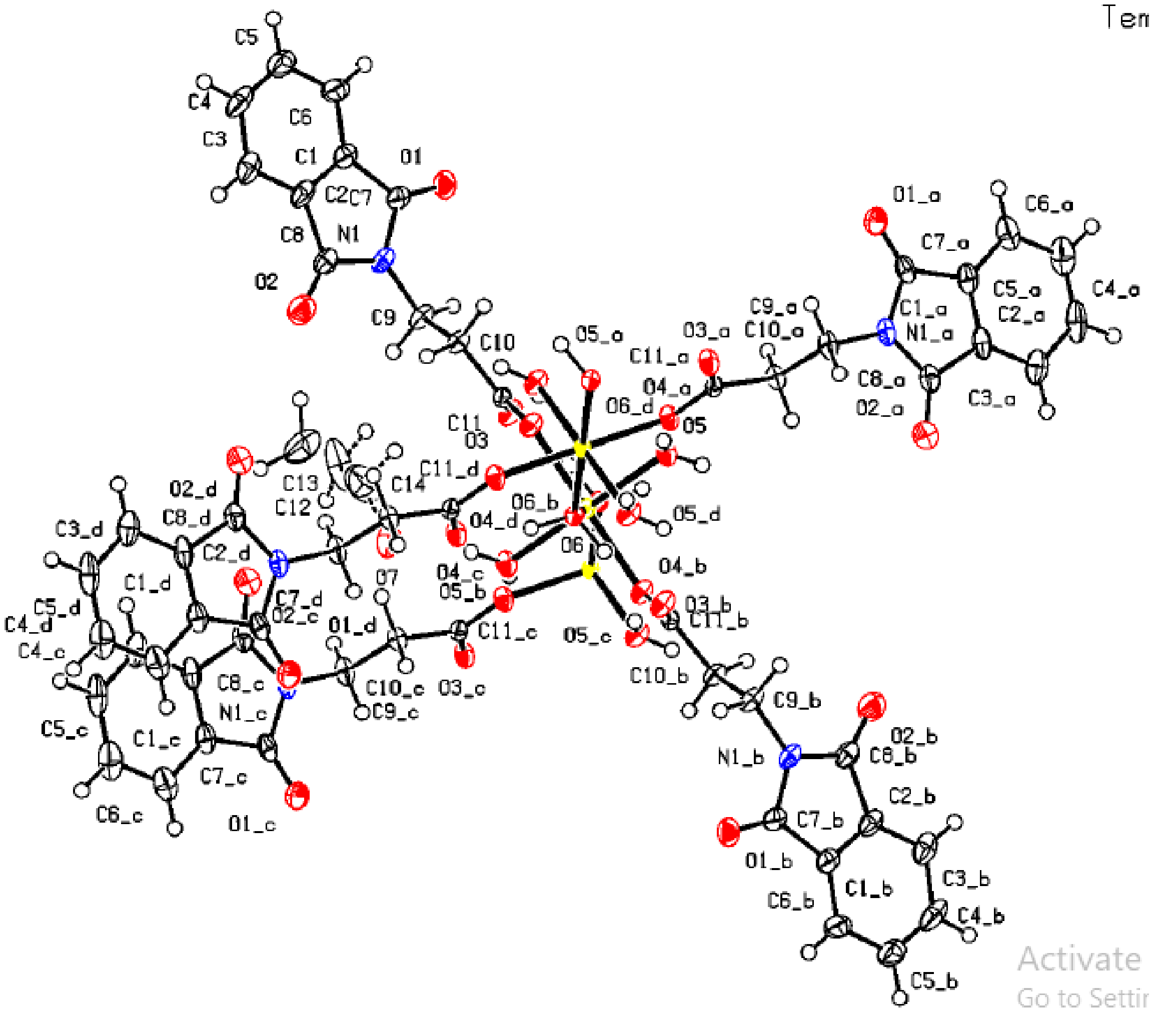

Fig. S26: Thermal ellipsoidal diagram of MOF **1**. 50% probability.

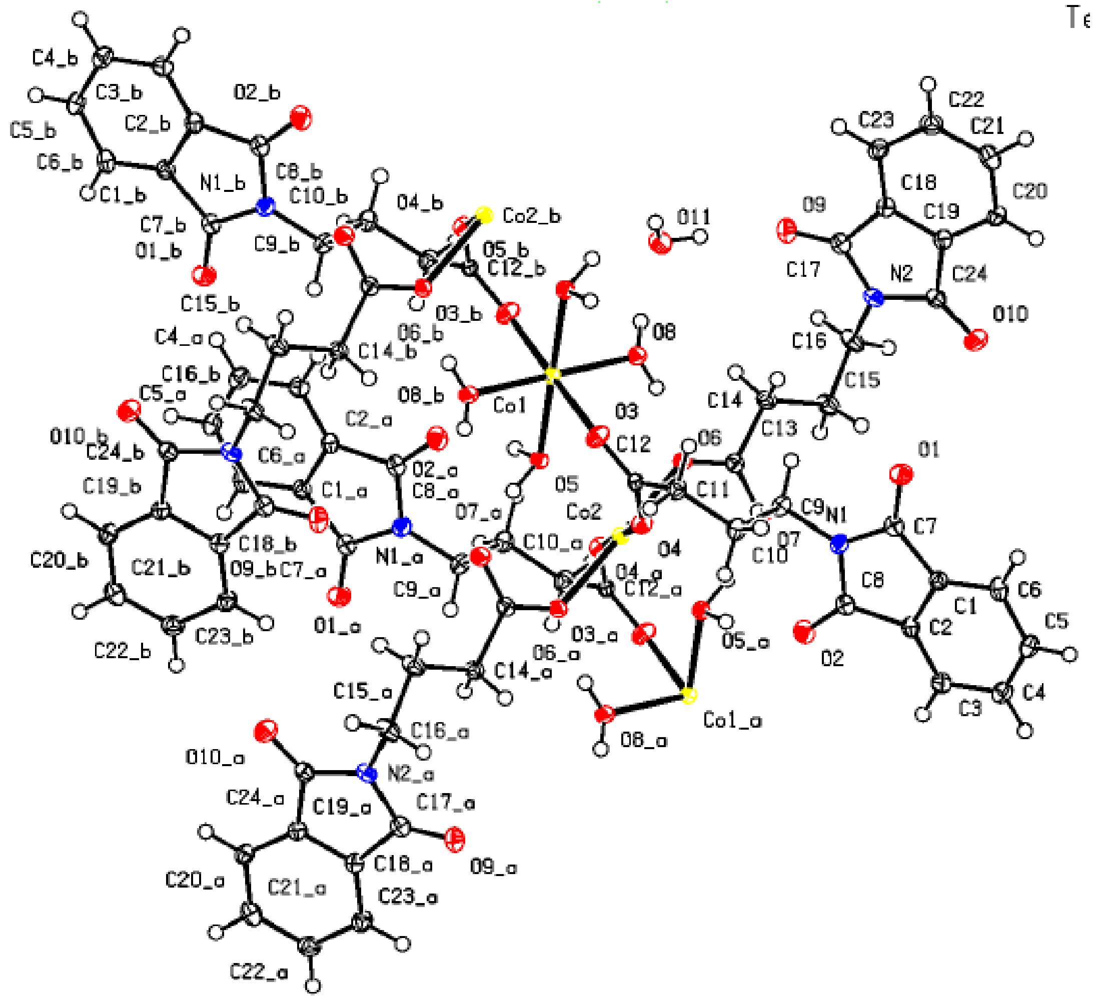

Fig. S27: Thermal ellipsoidal diagram of MOF **2.** 50% probability.

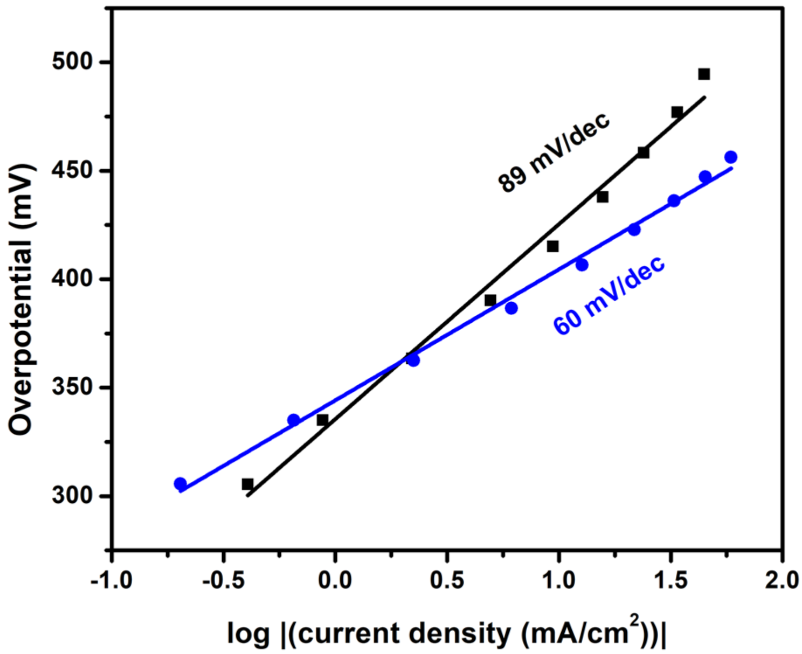

Fig. S28: The tafel slope value in a steady state of MOF **1** (black) and MOF **2** (blue).

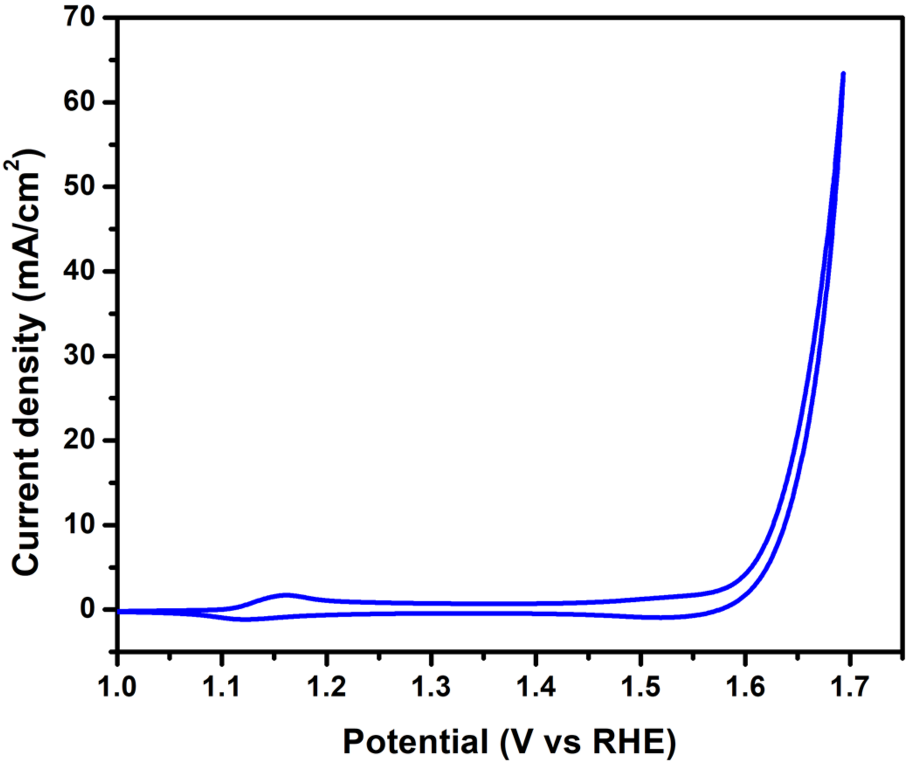

Fig. S29: CV of **MOF 1.**

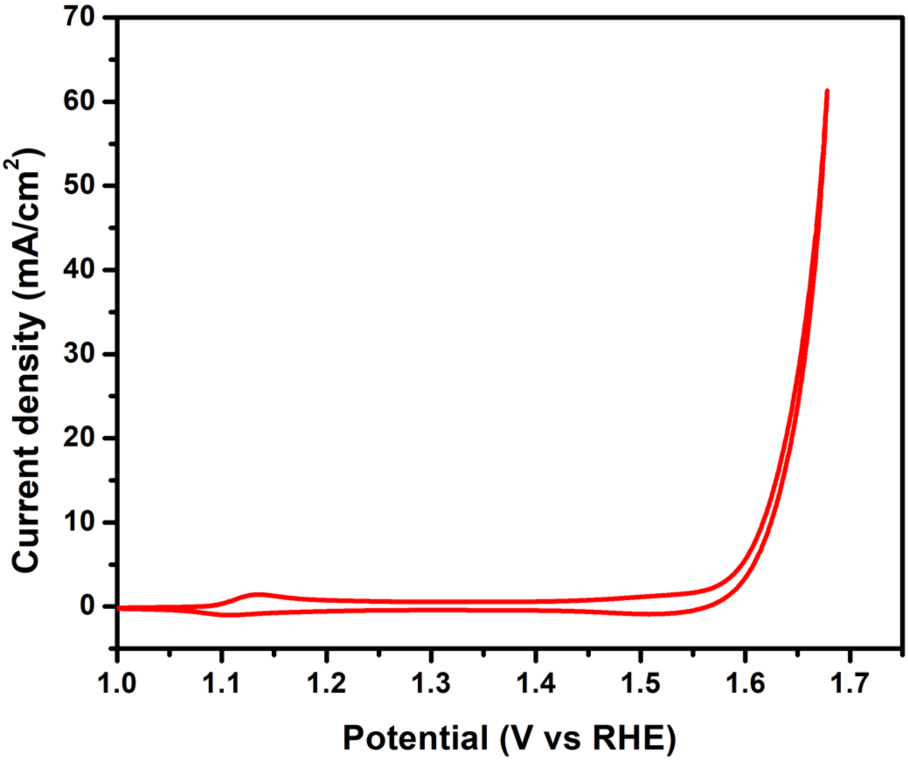

Fig. S30: CV of **MOF 2.**